Novel and Innovative Interface as Potential Active Layer in Chem-FET Sensor Devices for the Specific Sensing of Cs+

Volkan Kilinc, Catherine Henry-De-Villeneuve, Tin Phan Nguy, Yutaka Wakayama, Anne M Charrier, Jean-Manuel Raimundo

ACS APPLIED MATERIALS & INTERFACES

Research Article

www.acsami.org

Novel and Innovative Interface as Potential Active Layer in Chem-FET Sensor Devices for the Specific Sensing of Cs^+

Volkan Kilinc,[†,§] Catherine Henry-de-Villeneuve,[‡] Tin Phan Nguy,[†,§] Yutaka Wakayama,[§] Anne M. Charrier,*[,†] and Jean-Manuel Raimundo*[,†]

[†]Aix Marseille Univ, CNRS, CINAM, 13009 Marseille, France

[‡]Laboratoire de Physique de la Matière Condensée, Ecole Polytechnique, CNRS, IP Paris, 91128 Palaiseau, France

[§]International Center for Materials Nanoarchitectonics (WPI-MANA), National Institute for Materials Science (NIMS), 1-1 Namiki, 305-0044 Tsukuba, Japan

Supporting Information

ABSTRACT: An innovative novel interface has been designed and developed to be used as a potential active layer in chemically sensitive field-effect transistor (Chem-FET) sensor devices for the specific sensing of Cs^+. In this study, the synthesis of a specific Cs^+ probe based on calix[4]arene benzocrown ether, its photophysical properties, and its grafting onto a single lipid monolayer (SLM) recently used as an efficient ultrathin organic dielectric in Chem-FETs are reported simultaneously. On the basis of both optical and NMR titration experiments, the probe has shown high selectivity and specificity for Cs^+ compared to interfering cations, even if an admixture is used. Additionally, attenuated total reflectance mode Fourier transform infrared spectroscopy was successfully used to characterize and prove the efficient grafting of the probe onto a SLM and the formation of the innovative novel sensing layer.

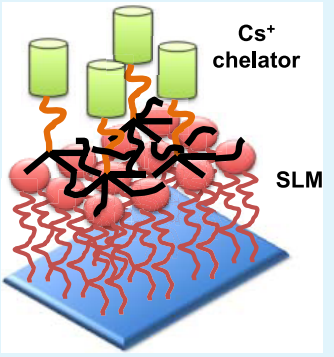

KEYWORDS: *lipid monolayers, ultrathin dielectric, sensors, cesium detection, calixarene*

INTRODUCTION

Ultrafast ions trace quantification methods have attracted tremendous interest in the last decades with the aim to be applicable for the detection of hazardous cations and anions. In this context, we have focused our investigation on the Cs^+ detection motivated both by the recent accidents in nuclear power plants, the frequent discharges from the nuclear reactors, and its uses in nuclear weapon testing. Additionally, cesium is used in food and drug sterilization processes; medicine therapies;[1] and many industrial applications such as optical glasses, photoelectric cells,[2] or ion propulsion systems. Radioactive cesium represents one of the most toxic elements that can be found in the flora and fauna[3,4] because it is easily displaced and incorporated in nature due to its high solubility in water, causing detrimental effects to the environment and human health.[5,6]

Hence, it is crucial to develop reliable and accurate methods for its detection and/or dosage to safeguard workers who are exposed daily to Cs^+, ensuring harmless uses and also safer working conditions. A rapid survey revealed that the most common method for the detection is based on the conventional ICP-MS technique.[7−10] Although accurate and sensitive, this technique is not suitable to achieve onsite and real-time measurements requiring expensive and sophisticated instrumentation as well as expert manpower. To overcome some of these drawbacks, chemists have devised optical methods based either on colorimetric or fluorometric assays by designing specific artificial hosts. Among them, 1,3-alternate calix[4]-arenes-based scaffolds topped with a crown ether have gained a lot of attention due to their well-defined structures exhibiting a cavity that fits perfectly with the cesium ionic radius.[11−13] Additionally, it is easy to tag them with fluorophores such as naphthalene or anthracene,[14] indanone,[15] or coumarin,[16,17] providing additional benefits in the modulation of optical properties.

However, for practical uses, they need to be integrated with devices that allow in situ real-time monitoring. To this end, we believe that the use of field-effect transistors constitutes a promising and reliable technology, which is worth and valuable for such purpose allowing miniaturization and wearable sensor systems. Moreover, we have recently demonstrated that engineered single lipid monolayers (SLMs) can be used as ultrathin dielectrics that have sensing properties with limits of detection down to the femtomole in chemically sensitive field-effect transistors (Chem-FET) sensors.[18−21]

Thus, in the line of our previous work, we will present herein the synthesis of a novel 1,3-alternate calix[4]arene host exhibiting high selectivity toward the foreseen Cs^+ analyte as shown by UV−vis and NMR titration analysis and its successful anchoring atop of a SLM generating an innovative

Received: October 11, 2019
Accepted: November 26, 2019
Published: November 26, 2019

DOI: 10.1021/acsami.9b18188
ACS Appl. Mater. Interfaces XXXX, XXX, XXX−XXX

sensing interface. The grafting process was monitored by an in situ Fourier transform infrared (FTIR) analysis using a homemade chamber that allows us to follow and characterize the direct functionalization of the SLM (Figure 1).

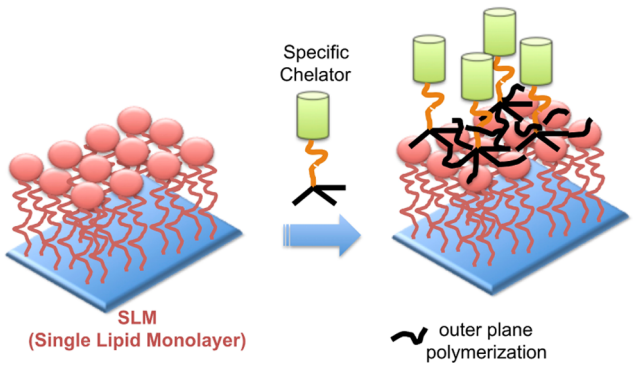

Figure 1. Schematic representation of an engineered SLM.

EXPERIMENTAL SECTION

Reagents and Analysis. 2-(2-Chloroethoxy)ethanol, catechol, and *p*-toluenesulfonyl chloride (TsCl) were purchased from TCI. Calix[4]arene and allyl bromide were purchased from Alfa Aesar. Karstedt's catalyst, Li^+, Na^+, K^+, Rb^+, Cs^+, and Mg^{2+} as chlorine salts, dimethylformamide (DMF), anhydrous acetonitrile (CH_3CN), methanol (MeOH), dichloromethane (DCM), tetrahydrofuran, anhydrous toluene, anhydrous 1,4-dioxane, K_2CO_3, NaOH, and Cs_2CO_3 were purchased from Sigma Aldrich. Column chromatography was performed using silica 60 M (0.04−0.063 mm) purchased from Macherey-Nagel.

Physicochemical Analysis. ^1H, ^{13}C, and ^{29}Si NMR spectra were recorded on a JEOL ECS spectrometer at 400 MHZ (^1H), 100 MHz (^{13}C), or 79 MHz (^{29}Si) at room temperature. NMR chemical shifts are given in ppm (δ) relative to Me_4Si with solvent resonances used as internal standards ($CDCl_3$: 7.26 ppm for ^1H and 77.2 ppm for ^{13}C). Mass spectrometry (MS) (ESI) analyses were performed on a SYNAPT G2 HDMS (Waters) spectrometer at the "Spectropole" of Aix-Marseille University.[22] This instrument was equipped with an electrospray ionization source (ESI) and a time-of-flight mass analyzer. The sample was ionized in electrospray positive mode with a tension of 2.8 kV, orifice tension of 50 V, and the N_2 rate of flow of 100 L/h. XRD was performed on a Rigaku Oxford Diffraction SuperNova diffractometer and measured at 203, 250, and 150 K under Cu radiation (λ = 1.54184 Å). Data collection, reduction, and multiscan ABSPACK corrections were performed with CrysAlisPro (Rigaku Oxford Diffraction). Using Olex2,[23] the structures were solved with the ShelXT structure solution program using Intrinsic Phasing and refined with ShelXL using least-squares minimization.[24] FTIR analysis was performed on an EQUINOX 55 spectrophotometer (Brucker, Germany) equipped with a liquid nitrogen-cooled mercury−cadmium telluride photovoltaic detector. The attenuated total reflectance (ATR) samples (FZ-purified Si(111) wafer of thickness 500−500 μm) were shaped as prisms with two opposite sides beveled at ∼45°. Their length (∼15 mm, for ca ∼30 internal reflections) was chosen to obtain wide-range FTIR spectra (1000−4000 cm^{-1}). Measurements were carried out in a N_2-purged chamber to minimize H_2O vapor and CO_2 absorption. Spectra were averaged over 150 scans (4 cm^{-1} resolution).

Physicochemical Measurements in Solution. UV−vis absorption spectra were obtained on a Jasco V-670 spectrophotometer. The electronic absorption maxima (λ_{max}) are directly extracted from absorption spectra of chelator **3** based solution. Under optimum conditions, the stoichiometry between the chelator **3** and different analytes were investigated by the molar ratio method[25,26] both in UV−vis and ^1H NMR techniques.

Synthesis of 1,3-Alternate 25,27-Bis-(1-allyloxy)-1,3-[1,2-bis[2-(2-oxyethoxy)ethoxy]phenylene]calix[4]arene (3). To a solution, under an argon atmosphere, of 1,3-diallyloxy calix[4]arene **1** (0.090 g, 0,180 mmol, 1.0 equiv) in 30 mL of anhydrous CH_3CN was added, in one portion, 0.234 g (0.730 mmol, 4.0 equiv) of cesium carbonate. The reaction mixture was stirred under reflux for 2 h prior to adding a solution of 0.120 g (0.198 mmol, 1.1 equiv) of **2** dropwise in 9 mL of anhydrous CH_3CN. The reaction mixture was refluxed for 2 days and then the reaction mixture was cooled down to room temperature. Solvent was removed under reduced pressure. The residue was taken up in 100 mL of CH_2Cl_2, and the organic phase was washed successively 2× with 60 mL of a 2 M aqueous HCl solution and then twice each with 50 mL of brine and 50 mL of water. The organic phase was dried over Na_2SO_4 and filtered, and the solvent was removed under vacuo. The residue was purified by column chromatography over SiO_2 (eluent: petroleum ether:EtOAc 8:2), yielding the titled compound in 61% as a colorless solid. Mp = 142 °C (uncorrected). ^1H NMR (400 MHz, $CDCl_3$): δ = 7.00 (d, 4H, ^3J = 7.5 Hz), 6.91 (dd, 8H, ^3J = 12.1, 4.8 Hz), 6.60 (td, 4H, ^3J = 7.5, 4.5 Hz), 5.65 (ddt, 2H, ^3J = 17.2, 10.6, 4.6 Hz), 4.97 (dd, 2H, ^3J = 10.7, 1.7 Hz), 4.84 (dd, 2H, ^3J = 17.3, 1.8 Hz), 4.09 (t, 4H, ^3J = 5.1 Hz), 4.03 (dd, 4H, ^3J = 4.1, 2.0 Hz), 3.60 (m, 20H). ^{13}C NMR (100 MHz, $CDCl_3$): δ = 138.23; 138.02; 131.16; 116.46; 115.64; 113.10; 112.21; 104.39; 104.29; 103.97; 97.95; 97.33; 52.93; 52.61; 52.34; 51.62 ppm. MS (ESI+) *m/z*: 772.3849 found for $[M + NH_4]^+$; calculated for $[M + NH_4]^+$; 772.3844. Elemental analysis for $C_{48}H_{50}O_8$+CH_3CN (%): calculated C, 75.45; H, 6.71; O, 16.08. Found C, 75.39; H, 6.67; O, 16,18.

Colorless crystals of **3** were obtained by slow diffusion of a CH_2Cl_2 solution into MeOH solvent, with the monoclinic space group *P*21 with *a* = 11.3911 (2) Å, *b* = 10.4981 (2) Å, *c* = 17.4878 (3) Å, α = 90°, β = 106.375 (2)°, γ = 90° at 293 K, with *Z* = 2 and *V* = 2006.45 (7) $Å^3$. The refinement of 7060 reflections and 505 parameters yielded R_1 = 0.0428 for all data (6283 reflections with $I > 2\sigma(I)$) (see the Supporting Information). Atomic coordinates, bond lengths, angles, and thermal parameters for **3** have been deposited at the Cambridge Crystallographic Data Centre (CCDC number: 1935509, DOI: 10.5517/ccdc.csd.cc22z1sx). Copies of the data can be obtained free of charge on application to CCDC, 12 Union road, Cambridge CB21EZ, UK. E-mail: deposit@ccdc.cam.ac.uk.

Synthesis of 1,3-Alternate 25-[(3-Triethoxy)-silyl-1-propyloxy]-27-(1-allyloxy)-1,3-[1,2-bis-[2-(2-oxyethoxy)-ethoxy]-phenylene]calix[4]arene (4). To a solution, under an argon atmosphere, of **3** (0.050 g, 0.066 mmol, 1.0 equiv) in 2 mL of anhydrous was added 0.027 mL (0.145 mmol, 2.2 equiv) of triethoxysilane, and the reaction mixture was stirred at room temperature for 20 min. The reaction vessel was placed in a glovebox and 0.020 mL of the Karstedt's catalyst was added dropwise. The reaction was warmed up to 50 °C and stirred for 12 h. The reaction mixture was cooled down to room temperature and filtered through Celite pad. Excess triethoxysilane and solvent were removed under reduced pressure. The product was used without further purification. ^1H NMR (400 MHz, $CDCl_3$): δ = 6.81 (m, 16H, H aromatics), 5.69 (m, 1H, H vinyl), 3.89 (m, 36H, CH_2), 1.25 (m, 9H, methyl), 0.94 (m, 2H, CH_2) NMR ^{29}Si ($CDCl_3$, 79 MHz): δ −100 (s, 1Si).

RESULTS AND DISCUSSION

The synthesis of the target chelator **3** is outlined in Scheme 1. Compound **3** was readily obtained from the cross-coupling of the ditosylate **2** and the calix[4]arene **1**[27,28] in CH_3CN at 80 °C in the presence of Cs_2CO_3 in 61% yield.[29]

The ditosylate **2** was prepared according to the reported literature procedures[30,31] from commercially available catechol, which was first alkylated with 2-(2 chloroethoxy)-ethanol in the presence of K_2CO_3 in DMF to form a diol intermediate in 47% yield (see Supporting Information (SI), Figure S1). The latter was subsequently treated with *p*-toluenesulfonyl chloride

DOI: 10.1021/acsami.9b18188
ACS Appl. Mater. Interfaces XXXX, XXX, XXX−XXX

Scheme 1. Synthesis of the Chelator 3

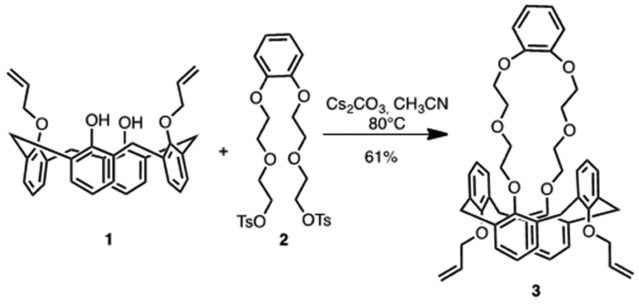

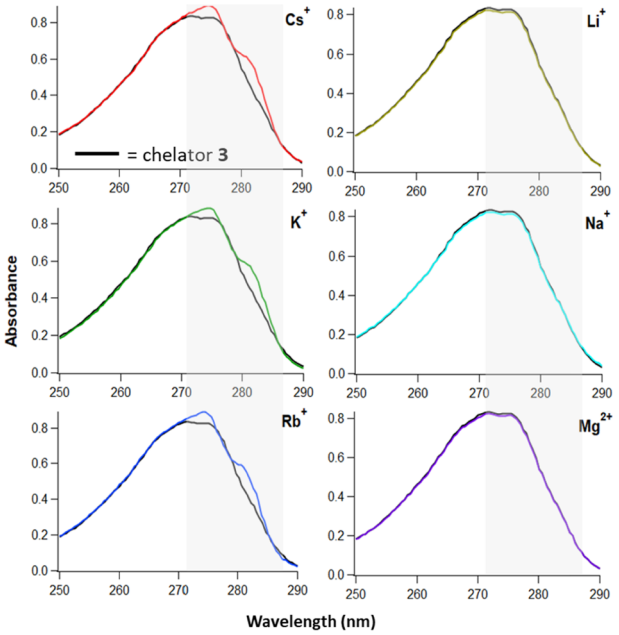

Figure 2. Optical properties of the receptor **3** (−) after addition of 1 equiv of Li^+ (light green line), Na^+ (sky blue line), K^+ (dark green line), Rb^+ (blue line), Cs^+ (red line), and Mg^{2+} (violet line) cations.

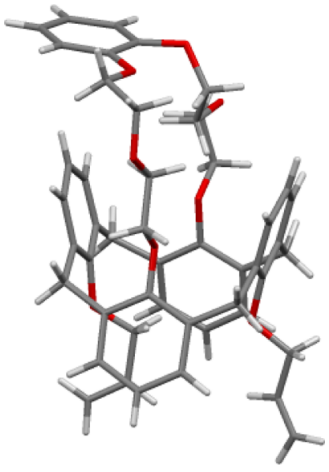

Figure 3. Crystal structure of **3** (C, gray, H, white, O, red).

in pyridine to afford the ditosylate **2** in 62% yield (see SI Figure S2).[32,33]

The optical properties, absorption, and fluorescence emission of the chelator **3** have been investigated in a solvent mixture MeOH/DCM (v/v, 1:1). Ultimately, the receptor exhibited poor fluorescence properties, and thereafter no further studies have been pursued by fluorescence spectroscopy. UV−vis absorption spectrum of the receptor **3** presents several absorption bands in the region 240−300 nm ascribed to the absorption of the benzene rings of both the calix[4]arene scaffold and the benzocrown ether. The cation-binding properties of the chelator **3** were screened by UV−vis spectroscopy with several putative competitive monovalent cations (Li^+, Na^+, K^+, Rb^+, Cs^+) and also with a divalent cation (Mg^{2+}) (Figure 2).

Job plots were performed using a solvent mixture of MeOH:DCM (SI Figure S7) and clearly indicate, for the

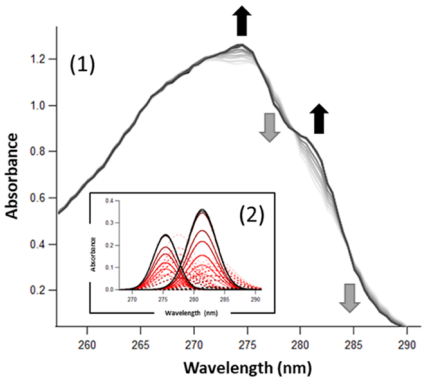

Figure 4. (1) Absorbance properties of the receptor **3** (−) upon the addition from 0 to 1 equiv of Cs^+ (light to dark). (2) (red line) Inset: evolution of the absorbance at λ of interest after a mathematical fitting. Full line corresponds to the black arrows, whereas dashed line corresponds to the gray arrows of (1).

Table 1. Association Constants (K_a) Determined in MeOH/DCM (1:1) at 293 K for the Host−Guest Complexes 3.X^{+a}

	K_a (10^3 M^{-1})	stoichiometry
Cs^+	6.024	1:1
K^+	2.825	1:1
Rb^+	2.288	1:1

[a]Not determined for Na^+, Li^+, and Mg^{2+}, as no complexation occurs.

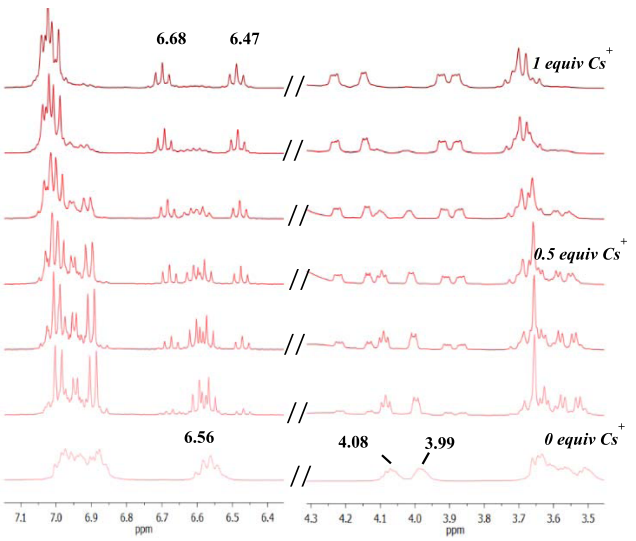

Figure 5. ^{1}H aromatic and aliphatic regions of **3** upon addition of 0 to 1 equiv of Cs^+ as chlorine salts in $CDCl_3$/MeOD (1:1) with traces of D_2O.

DOI: 10.1021/acsami.9b18188
ACS Appl. Mater. Interfaces XXXX, XXX, XXX−XXX

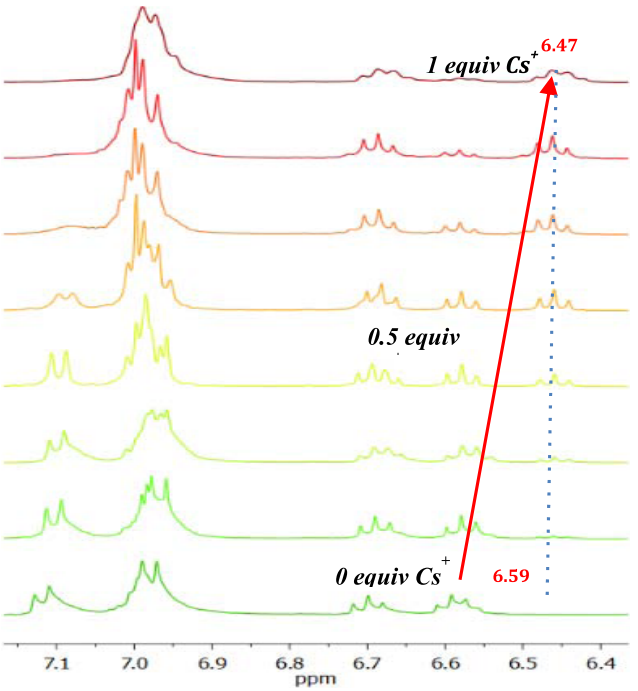

Figure 6. ^{1}H aromatic regions of **3.K$^+$** upon addition of 0 to 1 equiv of Cs^+ as chlorine salts in $CDCl_3$/MeOD (1:1) with traces of D_2O.

Scheme 2. Synthesis of the Host-Modified Molecule 4

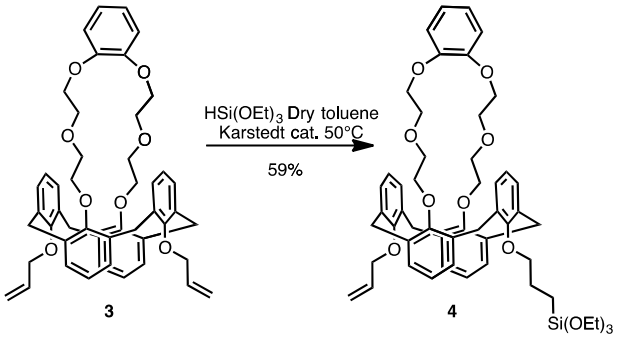

studied cations, the formation of a [1 + 1] complex **3.X$^+$**, which is in agreement with the results reported on similar scaffolds.[11−13] No further optical changes were observed after the addition of an excess of cations. Moreover, it is important to notice that even in competitive polar solvent such as MeOH, we observed for the cationic guest of interest, Cs^+, some interactions with **3** that allow its detection. Furthermore, minor optical changes upon the addition of the cationic guests constitute a proof that the host−guest interaction occurs predominantly in the crown ether part. This behavior was further confirmed by ^{1}H NMR titration experiments (vide infra) and is consistent with the crystallographic observations obtained from the X-ray structure of **3** (Figure 3 and SI Figure S3). Further examination of the cavity size from the X-ray structure revealed that the measured distances Cs^+−O (3.31 Å) and Cs^+−Ar_{calix} (3.44 Å) are in accordance with similar reported systems, indicating that the cavity of **3** is more suitable for the Cs^+ compared to that of the others.[34]

Greater optical changes were observed for Cs^+, K^+, and Rb^+, while much smaller variations are observed for others cations (Na^+, Li^+, and Mg^{2+}), with the spectra remaining almost unchanged. Upon addition of Cs^+, K^+, or Rb^+, an enhancement of the absorption bands centered at 275 and 281 nm was observed, highlighting the formation of the **3.X$^+$** complexes. It was anticipated that the presence of the benzene ring in the crown ether part could impart a reduction of the flexibility of the cavity, preventing the complexation of smaller cations such as Na^+, Li^+, and Mg^{2+}.

Although it is easy to differentiate between the ions interacting with the crown ether from those that cannot, due to the emergence of new peaks on the absorption spectra, it appears less obvious for Cs^+, K^+, and Rb^+ because they displayed similar behaviors. Thus, to have a more pronounced difference between these three cations, giving a positive signal, it is necessary to apply a fitting mathematical function taking into account the spectral modifications (Figure 4, inset and SI Figures S4−S6). For instance, upon the gradual addition of the Cs^+ cation, the variations of the absorption properties of **3** are associated with hyperchromic (at 275 and 281 nm) and hypsochromic effects (slightly blue-shifted from 277 to 275 nm and from 283 to 281 nm, respectively). These optical changes and the appearance of isobestic points attest undoubtedly to the ability of **3** to bind these cations. On the basis of these results, an approximate Hofmeister series can be settled, which follows approximately the radius of each cation: $Cs^+ > Rb^+ > K^+ > Na^+ > Li^+ \approx Mg^{2+}$.[35,36] Hence, association constants can be determined using the Benesi−Hildebrand method,[37,38] showing that **3** presents higher selectivity toward Cs^+ with a K_a = 6.024 × 10^3 M^{-1}, which is 3- or 2-fold higher than that toward K^+ (2.825 × 10^3 M^{-1}) and Rb^+ (2.288 × 10^3 M^{-1}), respectively (Table 1 and SI Figure S8).

To get further information on the chelating ability of **3**, ^{1}H NMR titration experiments were conducted in a mixture of deuterated $CDCl_3$/MeOD (1:1) solutions in the presence of traces of D_2O. By varying gradually the number of equivalents of each cation, it is clearly evidenced that the complexes **3.X$^+$** were formed. Indeed, both aromatic and aliphatic regions dramatically change as the number of equivalent of the added cation increases (Figure 5 and SI Figure S10).

Most of the protons in these two regions are affected, shifting progressively downfield or upfield, and are preeminent after the addition of 1 equiv of X^+. If an excess of cation X^+ is added, no further chemical shift is noticed in these two regions. Remarkably, in the ^{1}H aromatic region of the free host **3**, the multiplet centered at 6.56 ppm splits into two separated triplet signals (one at downfield and the second one at upfield) after the addition of 1 equiv of Cs^+. Moreover, in the ^{1}H aliphatic region, the two multiplets centered at 4.08 and 3.99 ppm, respectively, are more strongly affected upon complexation as four new signals are observed both at downfield and upfield compared to the two original multiplets. These findings indicate that the binding of Cs^+, as well as for the other cations takes place mostly in the crown ether part as reported on similar systems. The excellent selectivity toward cesium was found and ascribed to the combined electrostatic and cation−π interactions arising from cesium and oxygens of the crown ether or the aromatic rings of the scaffold, respectively.[11−13] In addition, the observed chemical shifts associated to the addition of the cations are greater when Cs^+ is added compared with when K^+ and Rb^+ are added, pinpointing that the host molecule **3** interacts more strongly with Cs^+ than with others.

As previously demonstrated, K^+ and Rb^+ are putative interfering analytes for Cs^+, even though they display lower affinity constants. To have more insights into that, guest-

DOI: 10.1021/acsami.9b18188
ACS Appl. Mater. Interfaces XXXX, XXX, XXX−XXX

Scheme 3. Modification of the Single Lipid Monolayer with 4

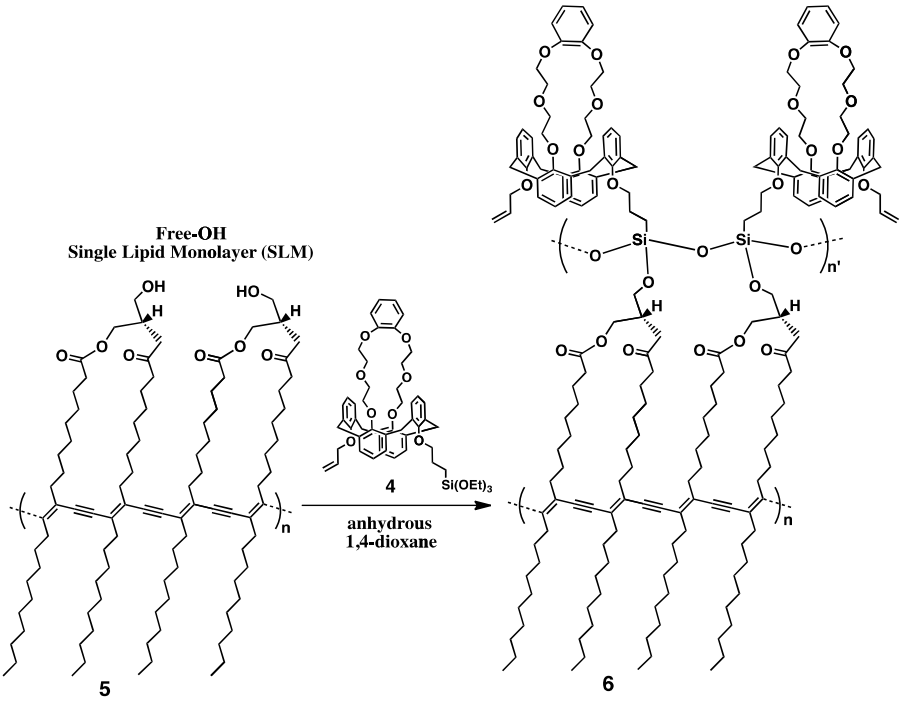

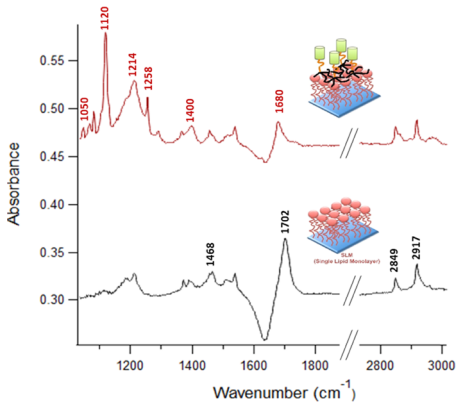

Figure 7. FTIR-ATR spectra of a functionalized lipid monolayer prior to (black plot) and after (red plot) reaction with **4**. The spectra were recorded in water. For both spectra, the reference is the silicon surface prior to the adsorption of the lipid monolayer.

displacement experiments were performed both by UV−vis and ^{1}H NMR (Figure 6 and SI Figure S10).

As exemplified, starting from complex **3.K**$^+$, the incremental addition of Cs^+ amounts leads to a dramatic change of the ^{1}H NMR spectrum. After the complete addition of 1 equiv of Cs^+, the obtained ^{1}H NMR spectrum appears to be the footprint of the one of the complexes **3.Cs**$^+$. This behavior reflects the greater ability of **3** to bind Cs^+ compared to K^+, as Cs^+ is able to replace K^+ guest. Moreover, if an admixture of cations is added to the chelator **3**, the obtained ^{1}H NMR corresponds to the one of **3.Cs**$^+$ when Cs^+ is added alone. Identical trends were observed by UV−vis experiments (see SI Figure S11).

These features constitute a clear proof that the host molecule **3** behaves as a specific and selective probe to the cesium cation even if competitive cations are present in the medium.

The intrinsic sensing properties of the novel chelator **3** with respect to Cs^+ led us to consider its possible use in a sensor device such as a Chem-FET. Nevertheless, prior to its implementation in a real device, it is required to graft it efficiently on a suitable surface. In this context, we have recently demonstrated that single lipid monolayer (SLM)[18−21] can be used as efficient organic dielectrics in field-effect transistors devices. Correspondingly, we have implemented a methodology that ensures us to have SLM with unprecedented mechanical and electrical properties.[39,40] Based on these relevant facts, we decided to functionalize the chelator **3** with an appropriate anchoring group to be grafted on an engineered SLM.

Thus, owing to our strategy, the triethoxysilane group was selected and used as an anchoring group. From **3**, this functional group can be easily introduced on the allyl part of the lower rim in one step using the Karstedt catalyst (Scheme 2).[41] The target functionalized compound **4** was obtained in 59% and used without further purification in the next step. Indeed, compound **4** might be also contaminated by the bis-silylated derivative, but this will not have any consequence on the grafting (see SI Figure S9).

First, a sample of a free-OH lipid was assembled on an edge-tailored silicon prism to form a self-assembled monolayer (SAM) and then polymerized within the plane of the monolayer by applying a protocol mastered by our group to form **5**.[18−21] The obtained SLM **5** was successfully characterized in situ prior to grafting the host compound **4** using a homemade infrared cell placed in an attenuated total reflectance mode Fourier transform infrared (ATR-FTIR) spectrophotometer (see SI Figure S12). The initiation and propagation of the polymerization in the outer plane was ensured by the polycondensation of triethoxysilane group with the ester group on the top of the SLM **5** (Scheme 3). It was performed by exposing the supported lipid monolayer to 0.25

DOI: 10.1021/acsami.9b18188
ACS Appl. Mater. Interfaces XXXX, XXX, XXX−XXX

mM solution of the substituted chelators **4** in anhydrous 1,4-dioxane.

FTIR spectra confirm the occurrence of the condensation reaction (Figure 7). After 1 h exposure in the chelator solution and rinsing, there was a decrease and a shift of the peak assigned to the carbonyl of the ester head groups ($\nu_{C=O}$ at 1702 cm^{-1}) and the appearance of new bands in the 1000−1300 cm^{-1} assigned to siloxane and/or calixarene bonding (ν_{Si-O}, ν_{C-O}), indicating the successful anchoring of the host molecule **4** on the surface. In addition, the spectra show that the intensity and position of the peaks corresponding to the aliphatic chains of the lipids (sym. ν_{CH_2} at 2849 cm^{-1} and asym. ν_{CH_2} at 2917 cm^{-1}) remain unchanged, indicating that the close-packed structure of the lipid monolayer is preserved.[42] All these observations are in favor of a successful anchoring of the host molecule at the surface of the SLM. This unique combination of this novel interface is of great interest to be used as an active layer in a Chem-FET. Preliminary results based on an electrolyte-gated organic field-effect transistor (EG-OFET) modified by the modified SLM **6** clearly evidence the detection of Cs^+ (see SI Figure S13). Measurements were performed in phosphate-buffered saline, i.e., in the presence of a competitive cation like K^+ or Na^+, highlighting the specificity of the chelator even in the presence of putative competitive ions. Thus, the tendencies observed from the free chelator **3** in solution are confirmed when the latter is grafted onto the SLM.

CONCLUSIONS

We reported herein the synthesis and characterization of a novel and innovative interface based on the combination of a calix[4]arene tethered with a benzocrown ether and a single lipid monolayer (SLM) that can be used as an effective sensing layer in a Chem-FET. Indeed, the newly appended calix[4]-arene possesses remarkable sensitivity and selectivity toward Cs^+ over other interfering cations, while SLM presents high mechanical and electrical properties as previously demonstrated. This unique combination of properties makes this innovative and novel interface a system of choice for the foreseen applications. Preliminary results conducted on an EG-OFET device have clearly demonstrated the effectiveness of this innovative interface for the specific detection of Cs^+ even in the presence of interferring ions. Further work and improvements are now under progress.

ASSOCIATED CONTENT

Supporting Information

The Supporting Information is available free of charge at https://pubs.acs.org/doi/10.1021/acsami.9b18188.

Synthesis of 1,3-diallyloxy calix[4]arene 1; synthesis of 1,2-bis[2-(2-hydroxyethoxy)ethoxy]benzene; synthesis of the intermediates for the synthesis of 3 (Figure S1); ^1H and ^{13}C NMR of the compound 3 (Figure S2); and X-ray structure of 3 (Figure S3) (PDF)

AUTHOR INFORMATION

Corresponding Authors

*E-mail: charrier@cinam.univ-mrs.fr (A.M.C.).

*E-mail: jean-manuel.raimundo@univ-amu.fr. Phone: +33 (0) 6 15 17 87 93 (J.-M.R.).

ORCID

Yutaka Wakayama: 0000-0002-0801-8884

Anne M. Charrier: 0000-0002-0205-1341

Jean-Manuel Raimundo: 0000-0003-4090-0479

Notes

The authors declare no competing financial interest.

ACKNOWLEDGMENTS

This research was performed under the framework of the Strategic International Collaborative Research Program (SICORP) and financially supported by the Japan Science and Technology Agency (JST) and l'Agence Nationale de la Recherche (ANR) Project No. ANR-16-JTIC-0003-01. We also thank Michel Giorgi (Spectropôle, Marseille) for the crystal structure determinations. V.K. thanks also the ANR agency for its doctoral financial support.

REFERENCES

(1) Pasternack, J. B.; Howell, R. W. RadNuc: A Graphical User Interface to Deliver Dose Rate Patterns Encountered in Nuclear Medicine with a 137Cs Irradiator. *Nucl. Med. Biol.* **2013**, *40*, 304−311.

(2) Yuan, S.; Chen, D.; Li, D.; Zhong, J.; Xu, X. In Situ Crystallization Synthesis of CsPbBr3 Perovskite Quantum Dot-Embedded Glasses with Improved Stability for Solid-State Lighting and Random Upconverted Lasing. *ACS Appl. Mater. Interfaces* **2018**, *10*, 18918−18926.

(3) Burger, A.; Lichtscheidl, I. Stable and Radioactive Cesium: A Review about Distribution in the Environment, Uptake and Translocation in Plants, Plant Reactions and Plants' Potential for Bioremediation. *Sci. Total Environ.* **2018**, *618*, 1459−1485.

(4) Murakami, M.; Ohte, N.; Suzuki, T.; Ishii, N.; Igarashi, Y.; Tanoi, K. Biological Proliferation of Cesium-137 through the Detrital Food Chain in a Forest Ecosystem in Japan. *Sci. Rep.* **2014**, *4*, No. 3599.

(5) Melnikov, P.; Zanoni, L. Z. Clinical Effects of Cesium Intake. *Biol. Trace Elem. Res.* **2009**, *135*, 1−9.

(6) Guy, R. H.; Hostynek, J. J.; Hinz, R. S.; Lorence, C. R. Metals and the Skin. In *Topical Effects and Systemic Absorption*; Marcel Dekker, Inc.: NY, 1999; p 431.

(7) Ohno, T.; Muramatsu, Y. Determination of Radioactive Cesium Isotope Ratios by Triple Quadrupole ICP-MS and its Application to Rainwater following the Fukushima Daiichi Nuclear Power Plant Accident. *J. Anal. Spectrom.* **2014**, *29*, 347−351.

(8) Zheng, J.; Tagami, K.; Bu, W.; Uchida, S.; Watanabe, Y.; Kubota, Y.; Fuma, S.; Ihara, S. 135Cs/137Cs Isotopic Ratio as a New Tracer of Radiocesium Released from the Fukushima Nuclear Accident. *Environ. Sci. Technol.* **2014**, *48*, 5433−5438.

(9) Zheng, J.; Bu, W.; Tagami, K.; Shikamori, Y.; Nakano, K.; Uchida, S.; Ishii, N. Determination of 135Cs and 135Cs/137Cs Atomic Ratio in Environmental Samples by Combining Ammonium Molybdophosphate (AMP)-selective Cs Adsorption and Ion-Exchange Chromatographic Separation to Triple-Quadrupole Inductively Coupled Plasma-Mass Spectrometry. *Anal. Chem.* **2014**, *86*, 7103−7110.

(10) Russell, B. C.; Warwick, P. E.; Croudace, I. W. Calixarene-based Extraction Chromatographic Separation of 135Cs and 137Cs in Environmental and Waste Samples Prior to Sector Field ICP-MS Analysis. *Anal. Chem.* **2014**, *86*, 11890−11896.

(11) Ungaro, R.; Casnati, A.; Ugozzoli, F.; Pochini, A.; Dozol, J.-F.; Hill, C.; Rouquette, H. 1,2-Dialkoxycalix[4]arene crown-6 in 1,3-alternate Conformation: Cesium-Selective Ligands using the Cation-arene Effect. *Angew. Chem., Int. Ed.* **1994**, *33*, 1506−1509.

(12) Lamare, V.; Dozol, J.-F.; Fuangswasdi, S.; Arnaud-Neu, F.; Thuéry, P.; Nierlich, M.; Asfari, Z.; Vicens, J. A new Calix[4]arene-bis(crown ether) Derivative Displaying an Improved Caesium over Sodium Selectivity: Molecular Dynamics and Experimental Inves-

DOI: 10.1021/acsami.9b18188
ACS Appl. Mater. Interfaces XXXX, XXX, XXX−XXX

tigation of Alkali-Metal Ion Complexation. *J. Chem. Soc., Perkin Trans. 2* **1999**, 271−284.
(13) Kim, S. K.; Vargas-Zunica, G. I.; Hay, B. P.; Young, N. J.; Delmau, L. H.; Masselin, C.; Lee, C. H.; Kim, J. S.; Lynch, V. M.; Moyer, B. A.; Sessler, J. L. Controlling Cesium Cation Recognition via Cation Metathesis within an Ion Pair Receptor. *J. Am. Chem. Soc.* **2012**, *134*, 1782−1792.
(14) Roper, E. D.; Talanov, V. S.; Gorbunova, M. G.; Bartsch, R. A.; Talanova, G. G. Optical Determination of Thallium(I) and Cesium(I) with a Fluorogenic Calix[4]arenebis(crown-6 ether) Containing One Pendent Dansyl Group. *Anal. Chem.* **2007**, *79*, 1983−1989.
(15) Yeon, Y.; Leem, S.; Wagen, C.; Lynch, V. M.; Kim, S. K.; Sessler, J. L. 3-(Dicyanomethylidene)indan-1-one-Functionalized Calix[4]arene−Calix[4]pyrrole Hybrid: An Ion-Pair Sensor for Cesium Salts. *Org. Lett.* **2016**, *18*, 4396−4399.
(16) Kumar, N.; Pham-Xuan, Q.; Depauw, A.; Hemadi, M.; Ha-Duong, N.-T.; Lefevre, J. P.; Ha-Thi, M.-H.; Leray, I. New Sensitive and Selective Calixarene-Based Fluorescent Sensors for the Detection of Cs+ in an Organoaqueous Medium. *New. J. Chem.* **2017**, *41*, 7162−7170.
(17) Pham-Xuan, Q.; Jonusauskaite, L.; Depauw, A.; Kumar, N.; Lefevre, J. P.; Perrier, A.; Ha-Thi, M. H.; Leray, I. New Water-Soluble Fluorescent Sensors Based on Calix[4]arene biscrown-6 for Selective Detection of Cesium. *J. Photochem. Photobiol., A* **2018**, *364*, 355−362.
(18) Nguyen, T. D.; El Zein, R.; Raimundo, J.-M.; Dallaporta, H.; Charrier, A.-M. Label Free Femtomolar Electrical Detection of Fe(iii) Ions with a Pyridinone Modified Lipid Monolayer as the Active Sensing Layer. *J. Mater. Chem. B* **2013**, *1*, 443−446.
(19) Nguyen, T. D.; Labed, A.; El Zein, R.; Lavandier, S.; Bedu, F.; Ozerov, I.; Dallaporta, H.; Raimundo, J.-M.; Charrier, A.-M. A Field Effect Transistor Biosensor with a γ-pyrone Derivative Engineered Lipid-Sensing Layer for Ultrasensitive Fe^{3+} ion Detection with Low pH Interference. *Biosens. Bioelectron.* **2014**, *54*, 571−577.
(20) Kenaan, A.; Nguyen, T. D.; Dallaporta, H.; Raimundo, J.-M.; Charrier, A.-M. Subpicomolar Iron Sensing Platform Based on Functional Lipid Monolayer Microarrays. *Anal. Chem.* **2016**, *88*, 3804−3809.
(21) Nguy, T. P.; Hayakawa, R.; Kilinc, V.; Petit, M.; Raimundo, J.-M.; Charrier, A.-M.; Wakayama, Y. Stable Operation of Water-Gated Organic Field-Effect Transistor Depending on Channel Flatness, Electrode Metals and Surface Treatment. *Jpn. J. Appl. Phys.* **2019**, *58*, SDDH02_1−SDDH02_5.
(22) For more information, see the website of Spectropôle from Aix Marseille University. https://fr-chimie.univ-amu.fr/spectropole/.
(23) Dolomanov, O. V.; Bourhis, L. J.; Gildea, R. J.; Howard, J. A. K.; Puschmann, H. OLEX2: A Complete Structure Solution, Refinement and Analysis Program. *J. Appl. Crystallogr.* **2009**, *42*, 339−341.
(24) Sheldrick, G. SHELXT—Integrated Space-Group and Crystal-Structure Determination. *Acta Crystallogr., Sect. A: Found. Adv.* **2015**, *71*, 3−8.
(25) Yoe, J. H.; Jones, A. L. Colorimetric Determination of Iron with Disodium-1,2-dihydroxybenzene-3,5-disulfonate. *Anal. Chem.* **1944**, *16*, 111−115.
(26) Job, P. *Spectrochemical Methods of Analysis*; Wiley Interscience: NY, 1971; p 346.
(27) Kim, J. S.; Cho, M. H.; Yu, I. Y.; Pang, J. H.; Kim, E. T.; Suh, I. H.; Oh, M. R.; Ra, D. Y.; Cho, N. S. Calix[4]arene Dibenzocrown Ethers as Cesium Ionophore. *Bull. Kor. Chem. Soc.* **1997**, *18*, 677−680.
(28) Kim, J. S.; Yu, I. Y.; Pang, J. H.; Kim, J. K.; Lee, Y.-I.; Lee, K. W.; Oh, W.-Z. New Calix[4]arene Dibenzocrown Ethers for Selective Sensing of Cesium Ion in an Aqueous Environment. *Microchem. J.* **1998**, *58*, 225−235.
(29) Ji, H. F.; Dabestani, R.; Brown, G. M.; Hettich, R. L. Synthesis and Sensing Behavior of Cyanoanthracene Modified 1,3-alternate calix[4]benzocrown-6: a New Class of Cs+ Selective Optical Sensors. *J. Chem. Soc., Perkin Trans. 2* **2001**, *4*, 585−591.
(30) Wright, K.; Melandri, F.; Cannizzo, C.; Wakselman, M.; Mazaleyrat, J. P. New Crown-Carrier Cα,α-Disubstituted Glycines Derived from α-methyl-(l)-DOPA. *Tetrahedron* **2002**, *58*, 5811−5820.
(31) Deutman, A. B. C.; Smits, J. M. M.; de Gelder, R.; Elemans, J. A. A. W.; Nolte, R. J. M.; Rowan, A. E. Strong Induced-Fit Binding of Viologen and Pyridine Derivatives in Adjustable Porphyrin Cavities. *Chem. - Eur. J.* **2014**, *20*, 11574−11583.
(32) Weber, E. Neutralliganden mit Tensidstruktur—Synthese, Komplexierung, Ionentransfer. *Liebigs Ann. Chem.* **1983**, *5*, 770−801.
(33) Surowiec, M.; Custelcean, R.; Surowiec, K.; Bartsch, R. A. Mono-ionizable Calix[4]arene-benzocrown-6 ligands in 1,3-Alternate Conformations: Synthesis, Structure and Silver(I) Extraction. *Tetrahedron* **2009**, *65*, 7777−7783.
(34) Sessler, J. L.; Kim, S.; Gross, D.; Lee, C.; Kim, J.; Lynch, V. Crown-6-calix[4]arene-Capped Calix[4]pyrrole: An Ion-Pair Receptor for Solvent-Separated CsF Ions. *J. Am. Chem. Soc.* **2008**, *130*, 13162−13166.
(35) Hofmeister, F. Zur Lehre yon der Wirkung der Salze. *Arch. Exp. Pathol. Pharmakol.* **1888**, *24*, 247−260.
(36) Lo Nostro, P.; Ninham, B. W. Hofmeister Phenomena: an Update on Ion Specificity in Biology. *Chem. Rev.* **2012**, *112*, 2286−2322.
(37) Benesi, H. A.; Hildebrand, J. H. J. A Spectrophotometric Investigation of the Interaction of Iodine with Aromatic Hydrocarbons. *J. Am. Chem. Soc.* **1949**, *71*, 2703−2707.
(38) Thordarson, P. Determining Association Constants from Titration Experiments in Supramolecular Chemistry. *Chem. Soc. Rev.* **2011**, *40*, 1305−1323.
(39) Kenaan, A.; Charrier, A.-M.; Lavandier, S.; Raimundo, J.-M. PCT International Applications. WO Patent WO2017064176A12017.
(40) Kenaan, A.; El Zein, R.; Kilinc, V.; Lamant, S.; Raimundo, J.-M.; Charrier, A.-M. Ultrathin Supported Lipid Monolayer with Unprecedented Mechanical and Dielectric Properties. *Adv. Funct. Mater.* **2018**, *28*, No. 1801024.
(41) Kim, Y.-J.; Jung, H.-S.; Lim, J.; Ryu, S.-J.; Lee, J.-K. Rapid Imaging of Latent Fingerprints Using Biocompatible Fluorescent Silica Nanoparticles. *Langmuir* **2016**, *32*, 8077−8083.
(42) Menzel, H.; Mowery, M. D.; Cai, M.; Evans, C. E. Fabrication of Noncovalent and Covalent Internal Scaffolding in Monolayer Assemblies Using Diacetylenes. *Macromolecules* **1999**, *32*, 4343−4350.

DOI: 10.1021/acsami.9b18188
ACS Appl. Mater. Interfaces XXXX, XXX, XXX−XXX

Supporting information

Novel and innovative interface as potential active layer in Chem-FET sensor devices for the specific sensing of Cs^+.

Volkan Kilinc,[1,3] Catherine Henry-de-Villeneuve,[2] Tin Phan Nguy,[1,3] Yutaka Wakayama,[3] Anne M. Charrier[1*] and Jean-Manuel Raimundo[1*]

[1] Aix Marseille Univ, CNRS, CINAM, 13009 Marseille, France

[2] Laboratoire de Physique de la Matière Condensée, Ecole Polytechnique, CNRS, IP Paris, 91128 Palaiseau, France

[3] International Center for Materials Nanoarchitectonics (WPI-MANA), National Institute for Materials Science (NIMS), 1-1 Namiki, Tsukuba 305-0044, Japan

*Corresponding authors email addresses: anne.charrier@univ-amu.fr; jean-manuel.raimundo@univ-amu.fr

S1: Synthesis of the intermediates for the synthesis of **3**.

Figure **S2**: ^1H and ^{13}C NMR of the compound **3**.

Figure **S3**: X-ray structure of **3**.

Figure **S4**: Fitting method of the UV-visible absorbance signal of the host **3** without (a) and with (b) cation.

Figure **S5**: Absorbance properties of the host **3** upon gradual addition of the [K^+].

Figure **S6**: Absorbance properties of the host **3** upon gradual addition of the [Rb^+].

Figure **S7**: Job plot experiments for the host molecule **3** and the guests Cs^+ (a), Rb^+ (b) and K^+ (c).

Figure **S8**: Determination of the affinity constants by the Benesi-Hildebrand method for complexes **3.Cs**$^+$(a) ; **3.Rb**$^+$ (b) and **3.K**$^+$.

Figure **S9**: ^1H NMR (400 MHz) and ^{29}Si NMR (79 MHz) in $CDCl_3$ for the molecule **4**.

Figure **S10**: ^1H NMR (400 MHz) titration experiments in MeOD/ $CDCl_3$ (1:1) of the host molecule **3** with CsCl in D_2O.

Figure **S11**: ^1H NMR (400 MHz) titration experiments in MeOD/ $CDCl_3$ (1:1) of the complex **3.K**$^+$ with CsCl in D_2O.

Figure **S12**: Experimental set-up and procedure monitored by *in situ* ATR-FTIR spectroscopy.

Figure **S13**: Electrical detection of Cs^+ using an EG-OFET modified by the SLM-**6**

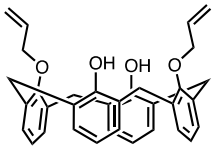

1

Synthesis of 1,3-diallyloxy calix[4]arene 1.[1] Under an Argon atmosphere, a mixture of 2.00 g (4.72 mmol, 1 equiv) of commercially available calix[4]arene and 0.72 g (5.20 mmol, 1.1 equiv) of K_2CO_3 in 50 mL of anhydrous CH_3CN were stirred under reflux for 2h. Then 1.17 g (9.68 mmol, 2.05 equiv) of allyl bromide was added dropwise to the reaction mixture. Reflux was continued for 2 days. After cooling, the solvent was removed under reduce pressure. The obtained residue was taken up in $CHCl_3$ (100 mL) and the organic phase was washed twice with 40 mL of a 2M aqueous HCl solution followed twice with 40 mL of water. The organic phase was dried over $MgSO_4$, filtered and evaporated in *vacuo*. The compound was purified by column chromatography over SiO_2 (eluent petroleum ether: DCM 1:1) yielding the titled compound in 62% as a white solid. ^{1}H NMR (400 MHz, $CDCl_3$): δ= 7.98 (s, 2H, OH); 7.09 (d, 4H, ^{3}J= 7.5 Hz); 6.94 (d, 4H, ^{3}J= 7.5 Hz); 6.78 (t, 2H, ^{3}J= 7.5 Hz); 6.69 (t, 2H, ^{3}J= 7.5 Hz); 6.30 (ddd, 2H, ^{3}J= 22.2, 10.4, 5.1 Hz, vinyl); 5.81 (dd, 2H, ^{3}J= 17.2, 1.5 Hz, vinyl); 5.45 (dd, 2H, ^{3}J= 10.6, 1.3 Hz, vinyl); 4.59 (d, 4H, ^{3}J= 5.0 Hz, vinyl-CH_2-Ar); 4.36 (d, 4H, ^{3}J= 13.1 Hz, Ar-CH_2-Ar); 3.42 (d, 4H, ^{3}J= 13.1 Hz, Ar-CH_2-Ar). ^{13}C NMR (100 MHz, $CDCl_3$): δ= 153.8; 152.3; 134.0; 133.4; 129.6; 129.1; 128.7; 126.1; 119.6; 118.5; 77.3; 32.0. The spectroscopic data were consistent with those previously published in literature.[1]

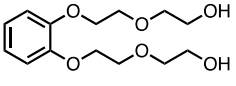

diol

Synthesis of 1,2-bis[2-(2-hydroxyethoxy)ethoxy]benzene.[2] To a solution under Argon atmosphere of 5.00 g (45.00 mmol, 1 equiv) of commercially available catechol **3** in 150 mL of anhydrous DMF was successively added at room temperature 63.00 g (0.45 mol, 10 equiv) of K_2CO_3 and 22.50 g (180 mmol, 4 equiv) of 2-(2-chloroethoxy)ethanol. The reaction mixture was heated to 80°C overnight under stirring. After cooling down the solvent was removed under reduced pressure to dryness. The residue was taken up in 150 mL of $CHCl_3$ and the organic phase was washed three times with 40 mL of a 0.5M aqueous NaOH solution followed by three times with 40 mL of water. The organic phase was dried over Na_2SO_4 and the solvent was removed in vacuo. The compound was purified by column chromatography over SiO_2 (hexane 6:4 EtOAc) yielding the titled compound in 47% as an orange oil.^{1}H NMR (400 MHz, $CDCl_3$): δ= 6.90 (d, 4H, ^{3}J= 1.9 Hz); 4.15 (dd, 4H, ^{3}J= 5.4, 3.5 Hz); 3.89 (m, 4H); 3.74-3.67 (m, 8H). The spectroscopic data were consistent with those previously published in literature.[2]

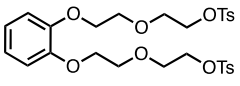

2

Synthesis of 1,2-bis[2-[2-[[(4-tolyl)sulfonyl]oxy]ethoxy]ethoxy]benzene 2.[2]

To a solution of 2.50 g (6.30 mmol, 1 equiv) of the **diol** in 6.25 mL of THF was added an aqueous solution of NaOH (1.23 g (30.00 mmol, 4.8 equiv) in 6.25 mL of water). The new solution was cooled down to 0°C and a solution of 3.67 g (19 mmol, 3 equiv) of p-toluenesulfonyl chloride in 8.75 mL of THF was added dropwise over a period of 1 hour. After addition, the reaction mixture was stirred a further hour at 0°C, then 25 mL of a 25% aqueous solution of HCl was added to quenched the reaction. The organic phase was extracted twice with 50 mL of DCM. The organic phase was then successively washed twice with 25 mL of water, twice of a 0.5M aqueous solution of $NaHCO_3$ and twice with 25 mL of water. The organic phase was dried over $CaCl_2$ and the solvent was removed under reduced pressure. The residue was purified by column chromatography over SiO_2 using a mixture of petroleum ether – EtOAc (80:20) as eluent. ^{1}H NMR ($CDCl_3$, 400 MHz) : δ 7.81 (d, 4H, ^{3}J= 8.2 Hz), 7.32 (d, 4H, ^{3}J= 8.1 Hz), 6.92 (m, 4H), 4.20 (t, 4H), 4.09 (t, 4H), 3.79 (q, 8H, ^{3}J= 5.7 Hz), 2.43 (s, 6H). The spectroscopic data were consistent with those previously published in literature.[2]

Synthesis of **1** according to: 1) a) Kim, J. S.; Cho, M. H.; Yu, I. Y.; Pang, J. H.; Kim, E. T.; Suh, I. H.; Oh, M. R.; Ra, D. Y.; Cho, N. S. *Bull. Kor. Chem. Soc.* **1997**, *18*, 677-680; b) Kim, J. S.; Yu, I. Y.; Pang, J. H.; Kim, J. K.; Lee, Y.-I.; Lee, K. W.; Oh, W.-Z. *Microchem. J.* **1998**, *58*, 225-235.

Synthesis of the diol and **2** according to: 2) a) Wright, K.; Melandri, F.; Cannizzo, C.; Wakselman, M.; Mazaleyrat, J. P. *Tetrahedron* **2002**, *58*, 5811-5820; b) Deutman, A. B. C.; Smits, J. M. M.; de Gelder, R.; Elemans, J. A. A. W.; Nolte, R. J. M.; Rowan, A. E. *Chem. Eur. J.* **2014**, *20*, 11574-11583.

S1 Synthesis of the intermediates for the synthesis of **3** according to reported procedures[1,2]

(a)

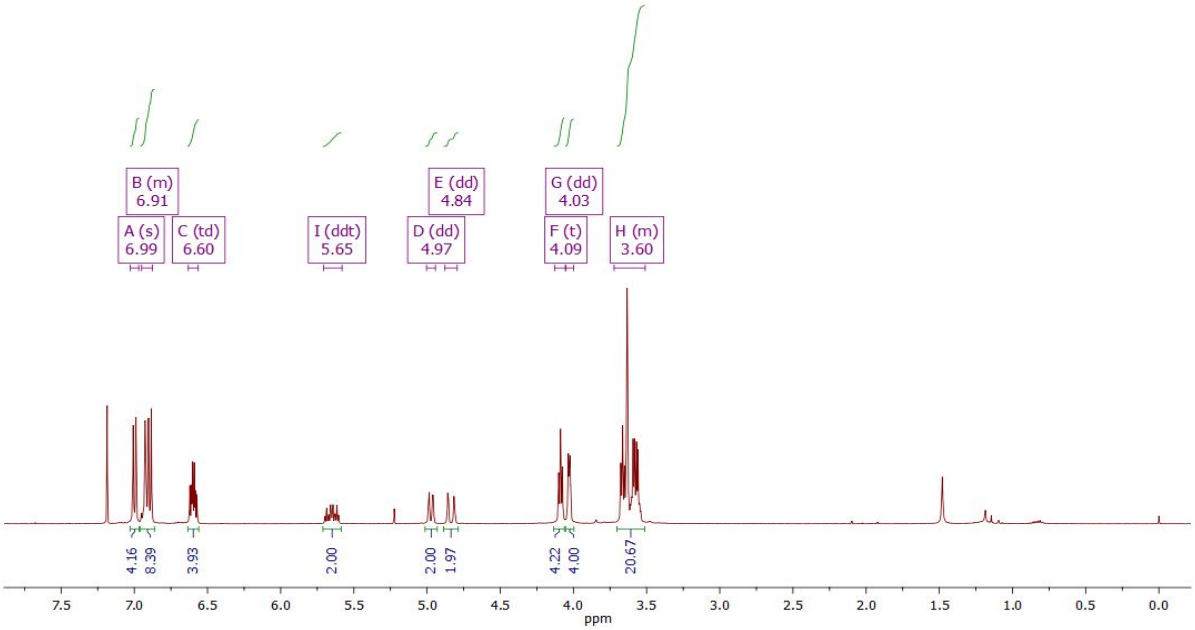

(b)

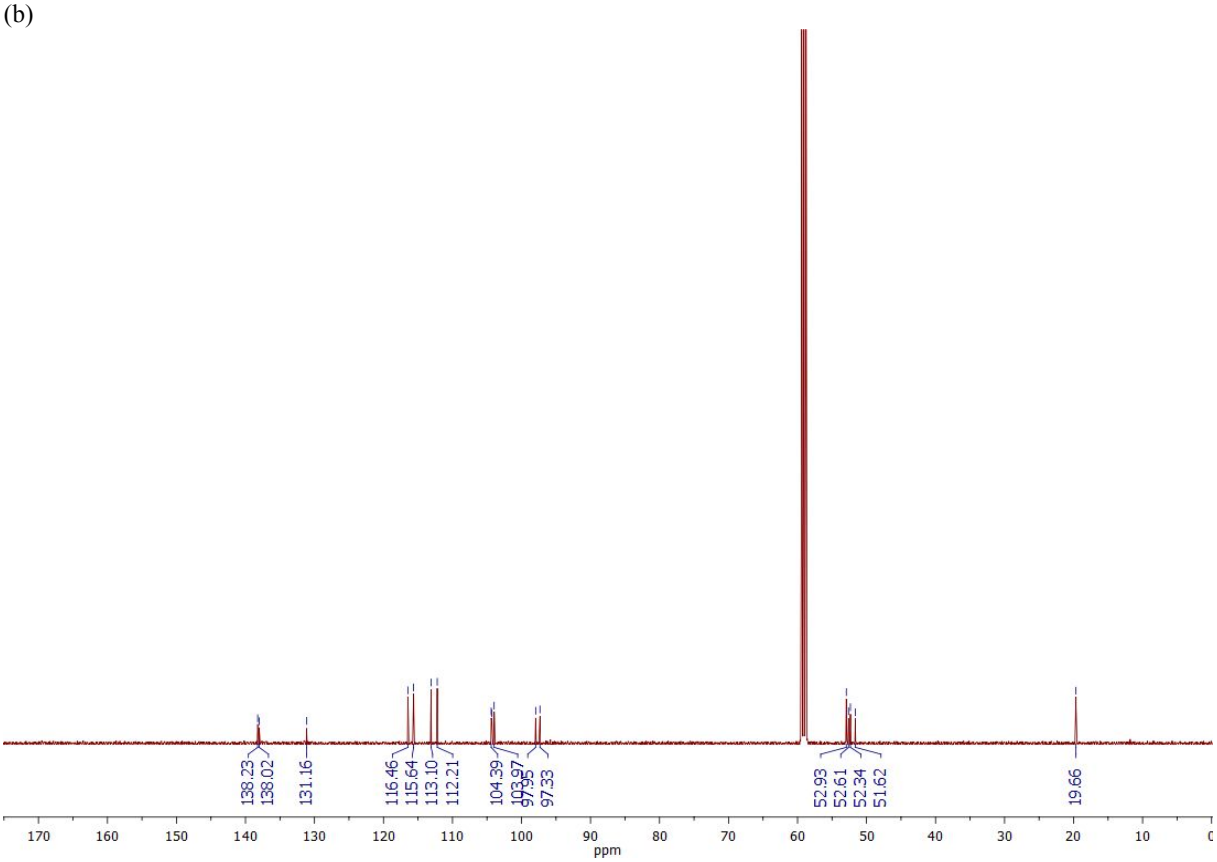

Figure **S2**: ^{1}H NMR (a) and ^{13}C NMR (b) respectively at 400 MHz and 100 MHz in $CDCl_3$ of the compound **3**

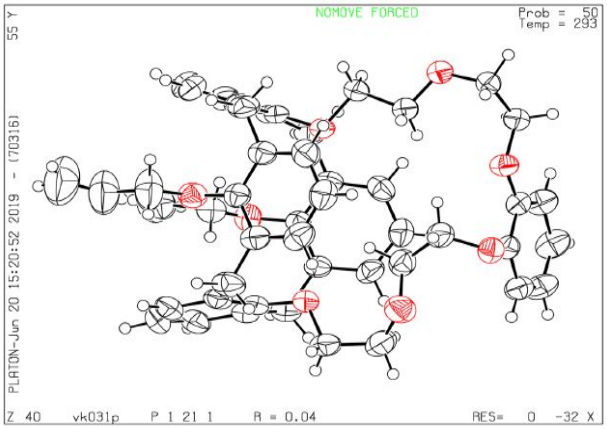

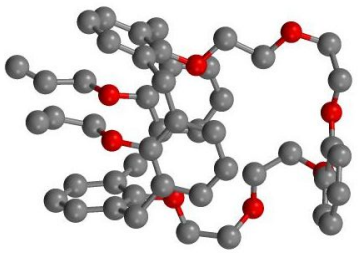

```
Bond precision:      C-C = 0.0056 A              Wavelength=1.54184
Cell:          a=11.3911(2)    b=10.4981(2)    c=17.4878(3)
               alpha=90        beta=106.375(2) gamma=90
Temperature
:              293 K
                    Calculated                  Reported
Volume              2006.45(7)                  2006.45(7)
Space group         P 21                        P 1 21 1
Hall group          P 2yb                       P 2yb
Moiety formula      C48 H50 O8                  C48 H50 O8
Sum formula         C48 H50 O8                  C48 H50 O8
Mr                  754.88                      754.88
Dx,g cm-3           1.250                       1.249
Z                   2                           2
Mu (mm-1)           0.676                       0.676
F000                804.0                       804.0
F000'               806.43
h,k,lmax            13,12,21                    13,12,21
Nref                7757[ 4103]                 7060
Tmin,Tmax           0.823,0.960                 0.739,1.000
Tmin'               0.816
Correction method= # Reported T Limits: Tmin=0.739
Tmax=1.000 AbsCorr = MULTI-SCAN
Data completeness= 1.72/0.91    Theta(max)= 71.213
R(reflections)= 0.0428( 6283)      wR2(reflections)= 0.1238( 7060)
S = 1.025              Npar= 505
```

Figure **S3** : X-ray structure of **3.** Crystals, stuitable for single crystal x-ray analysis were obtained by slow evaporation of a solution of **3** in CH_2Cl_2 into a methanolic solution. Crystallographic analysis shows that **3** crystallizes in the monoclinic space group P21.

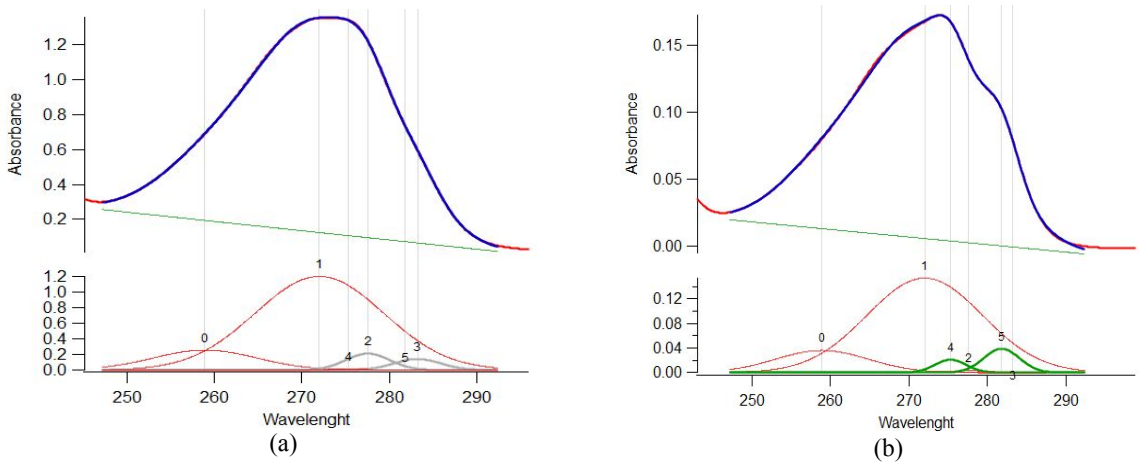

Figure **S4**: Fitting of the UV-visible absorbance signal of the chelator **3** without (a) and with (b) cation. All the spectra were fitted using a set of Gaussians after removal of the background.

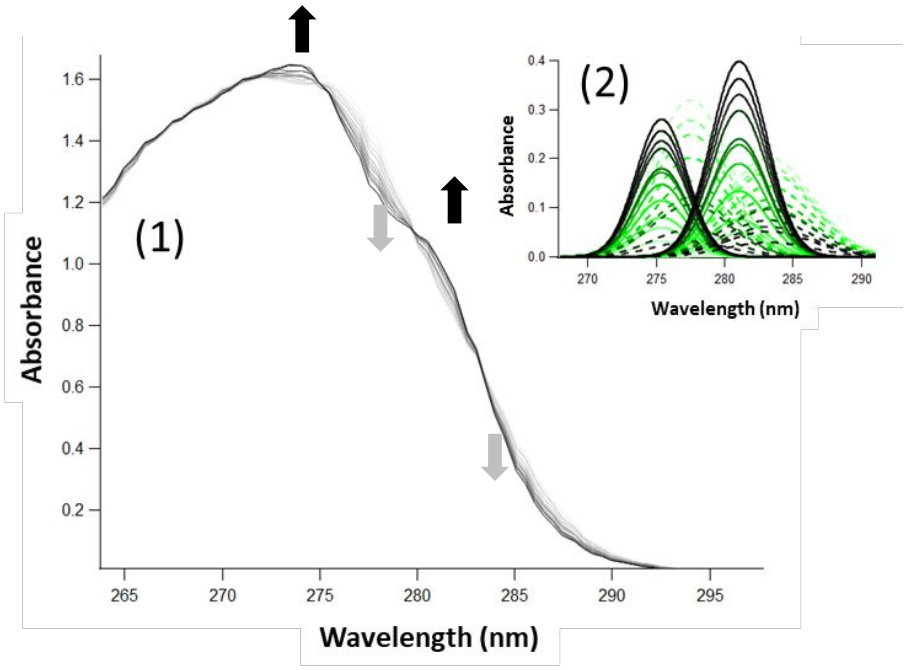

Figure **S5**: Absorbance properties of the host **3** upon gradual addition of the [K^+] up to 1 equiv (light to dark grey). Inset: Evolution of the absorbance at λ of interest after fitting the spectra with a set of Gaussians. The absorption properties of **3** are associated with hyper chromic (at 275 nm and 281 nm) and hypsochromic effects respectively (slightly blue-shifted from 277 to 275 nm and from 283 to 281 nm).

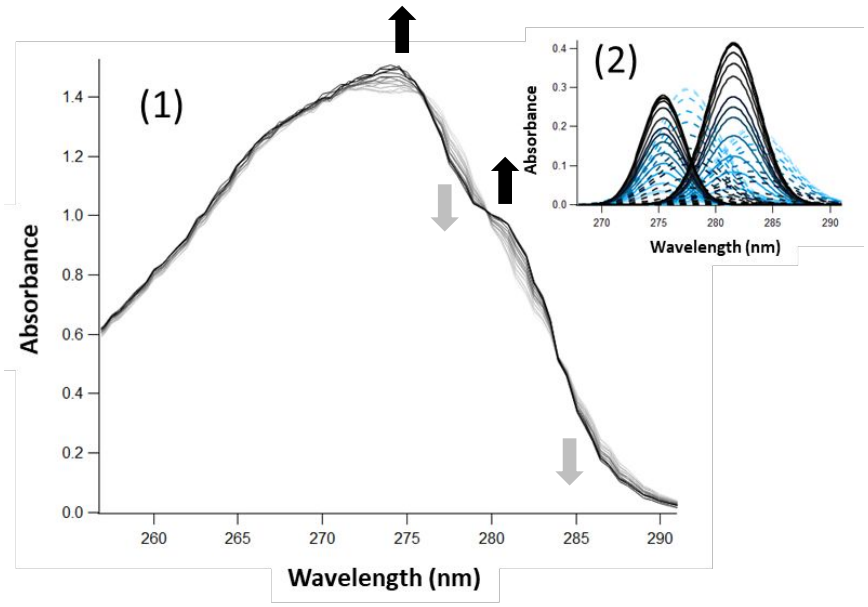

Figure **S6**: Absorbance properties of the host **3** upon gradual addition of the [Rb^+] up to 1 equiv (light to dark grey). Inset: Evolution of the absorbance at λ of interest after fitting the spectra with a set of Gaussians. The absorption properties of **3** are associated with hyperchromic (at 275 nm and 281 nm) and hypsochromic effects respectively (slightly blue-shifted from 277 to 275 nm and from 283 to 281 nm

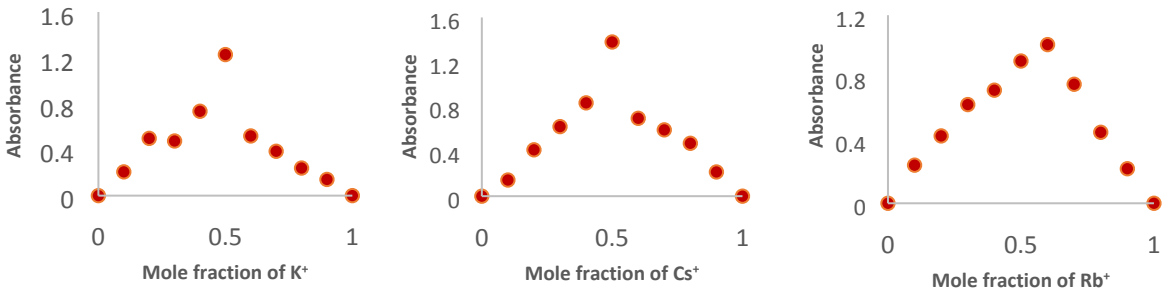

(a) (b) (c)

Figure **S7**: Job plot experiments for the host molecule **3** and the guests K^+ (a), Cs^+ (b) and Rb^+ (c).

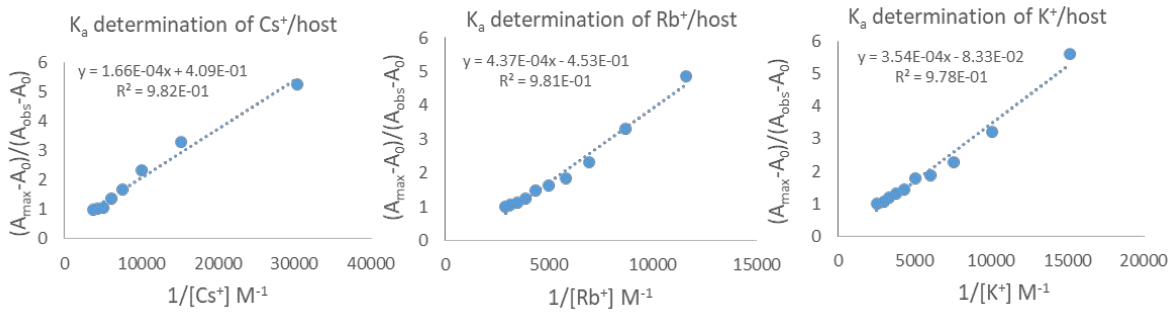

(a) (b) (c)

Figure **S8**: Determination of the affinity constants by the Benesi-Hildebrand method for complexes **3.Cs**$^{+}$(a) ; **3.Rb**$^{+}$ (b) and **3.K**$^{+}$.

a)

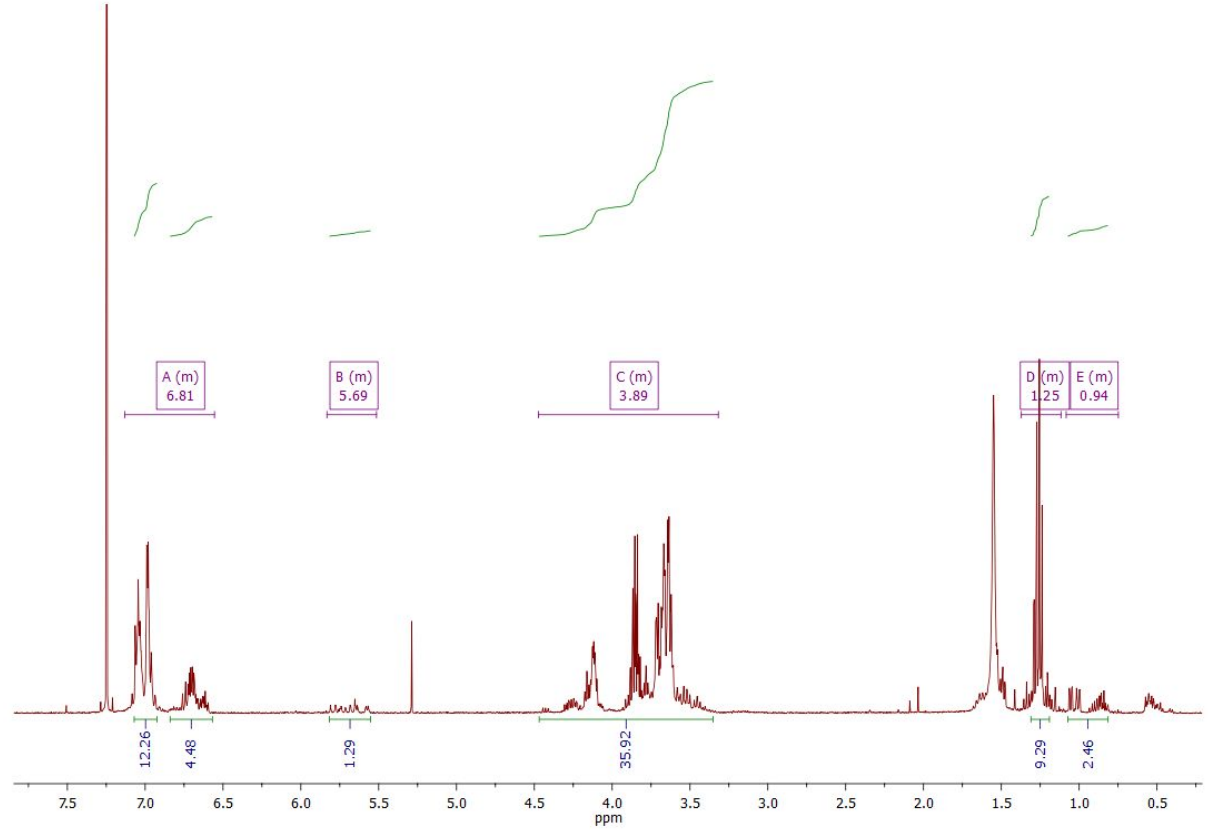

b)

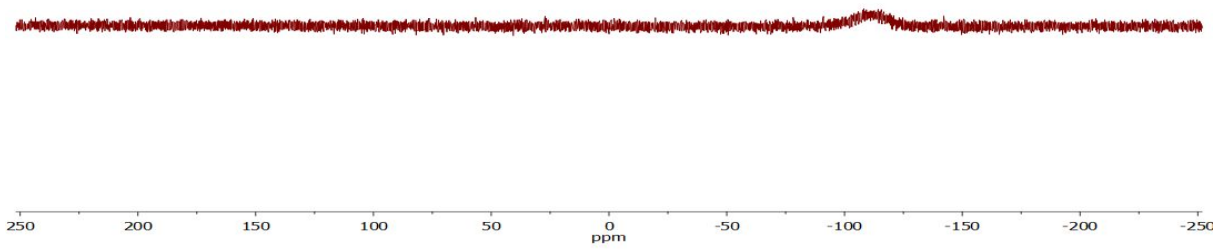

Figure **S9**: a) ^{1}H NMR (400 MHz) and b) ^{29}Si NMR (79 MHz) in $CDCl_3$ for the molecule **4**.

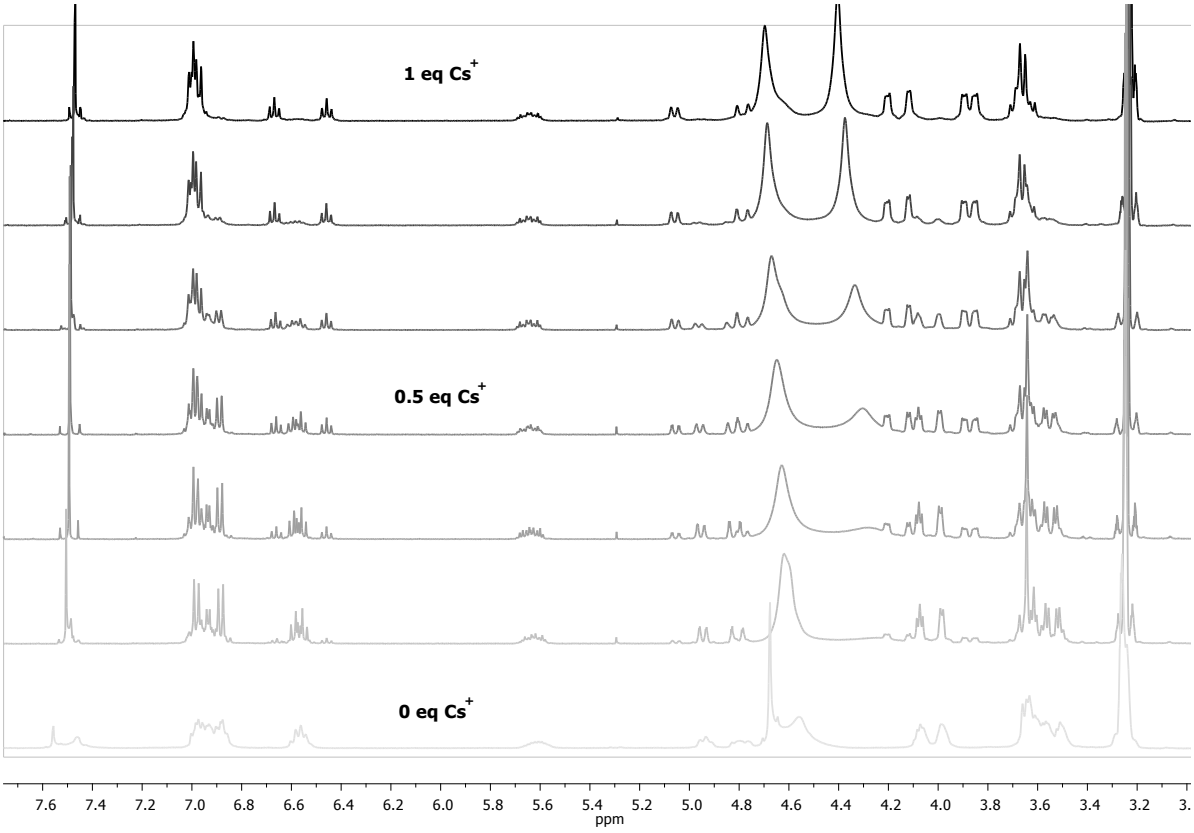

Figure **S10**: ^{1}H NMR (400 MHz) titration experiments in MeOD/ $CDCl_3$ (1:1) of the host molecule **3** with CsCl in D_2O.

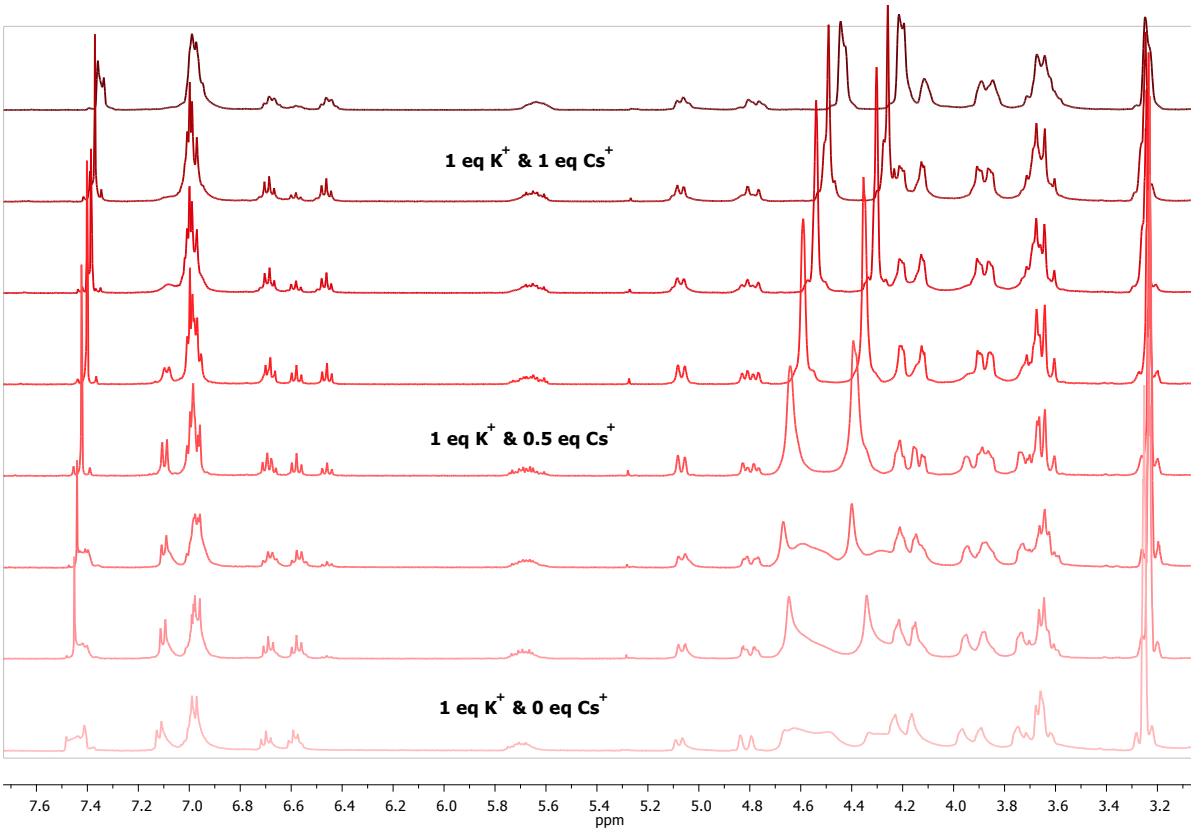

Figure **S11**: ^{1}H NMR (400 MHz) titration experiments in MeOD/ $CDCl_3$ (1:1) of the complex **3.K**$^{+}$ with CsCl in D_2O.

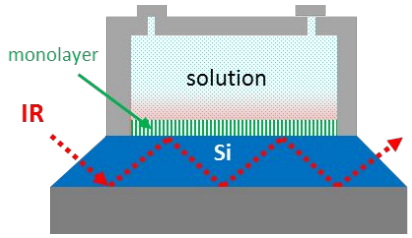

The Si sample was shaped as prism with two opposite edges beveled at 45° to guide the IR beam into the silicon such to have total reflection at the silicon/air (or solution) interface. When the IR beam is reflected at the Silicon/air or solution interface, the evanescent wave generated outside the silicon is absorbed by molecular species nearby the surface giving rise to a diminution of the IR intensity.

For *in situ* experiments, a close cell with a circular aperture (O-Ring diameter 10 mm, exposed area 0.8 cm^2) was pressed against the silicon prism and filled with the solution. The reference spectrum (bare Si surface prior to adsorption of the lipid ML) was recorded with the surface exposed to water. The lipid monolayer was then prepared by exposing the silicon surface to a lipid solution (0.3 mM in water). The surface in contact with the lipid solution was first cool down and then progressively warm up to form a dense and close-packed lipid monolayer according to a procedure previously reported by us. The surface was finally rinsed and the spectrum of the *Si-Lipid monolayer* surface recorded in water (black plot on the Figure **7**). For the anchoring of the chelators, the cell was emptied and dry carefully by Ar flowing. Then the surface was exposed to the chelator **4** solution (0.25 mM in anhydrous 1,4-dioxane) and the reaction let to proceed for 1 hour. The surface was afterwards rinsed copiously and the spectrum of the modified surface recorded in water (red plot on the Figure **7**).

Figure **S12**: Experimental set-up and procedure monitored by *in situ* ATR-FTIR spectroscopy.

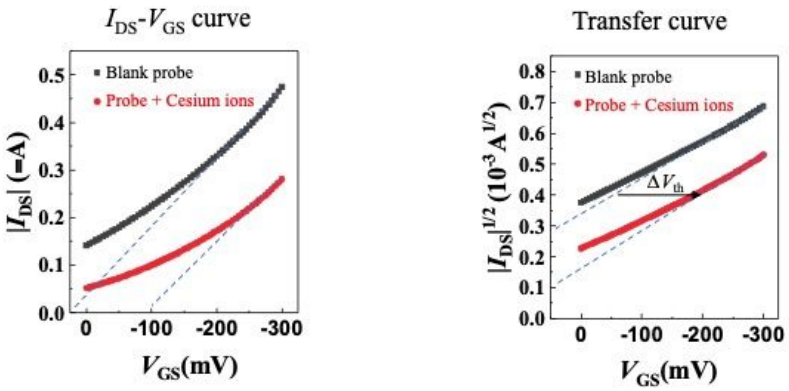

Figure **S13**: Electrical detection of Cs^+ using an EG-OFET modified by the SLM-**6**

The cesium probes were grafted on electrolyte gated organic field effect transistor (EG-OFET) functionalized by lipid monolayer for preliminary sensing experiments. The cesium ions were dissolved in DI-water to obtain a solution at 1 nM concentration. For sensing characterization, the shift of V_{th} of EG-OFET was used as an output signal. The V_{th} was extracted from the drain current (I_{DS})-gate voltage (V_{GS}) curve of EG-OFET. The phosphate-buffered solution (PBS) with a fixed pH of 6.86 was used as an electrolyte gate to evaluate the performance of EG-OFET. The gate voltage was swept from 0 V to −0.3 V at a fixed drain voltage of – 0.3 V.

Firstly, the sample with blank probes was measured in 200 µl of 1X PBS (~0.15 M) to get reference curve. Then, 100 µL of solution of 1 nM cesium ion was dropped on samples for 5 minute. Then, the sample was successively rinsed by DI-water and PBS. Finally, we obtained the I_{DS}-V_{GS} of EG-OFET after exposing to cesium ion.

Figure showed a clearly shift of I_{DS}-V_{GS} curve after the sample exposing to cesium ions. This means that cesium ions was captured by our probes and caused the change of I_{DS}-V_{GS} curve. Additionally, this capture occurred even in the presence of interfering ions (K^+, Na^+) in PBS. This result indicates that our designed probe has a high potential for cesium detection in interfering medium.